J. Phys. F: Met. Phys. **15** (1985) 809–834. Printed in Great Britain

Roughening transition of high-index crystal faces: the case of copper

J Villain†, D R Grempel‡ and J Lapujoulade§

† Centre d'Etudes Nucléaires de Grenoble, Département de Recherche Fondamentale, Laboratoire de Diffraction Neutronique, 85 X, F-38041 Grenoble Cédex, France
‡ Institut Laue–Langevin, 156 X, F-38042 Grenoble Cédex, France
§ Centre d'Etudes Nucléaires de Saclay, Service de Physique des Atomes et des Surfaces, F-91191 Gif-sur-Yvette Cédex, France

Received 24 April 1984, in final form 29 October 1984

Abstract. The thermal variation of atomic beam diffraction intensities on $(1, 1, 2n+1)$ faces of Cu is discussed for large n. The dramatic decrease of intensity at about 600 K is attributed to a roughening transition, above which the steps are fuzzy. The steps are assumed to repel themselves with a repulsion energy proportional to $(2n+1)^{-2}$, of elastic or electrostatic nature or both. The main parameter of the theory is the energy W_0 of a kink on a step. Experimental data are consistent with a value of W_0 between 0.2 and 0.3 eV, in agreement with very rough theoretical evaluations. Predictions are presented concerning the lineshape of diffraction spectra in the high-temperature rough phase, where intensities cannot be written as delta functions. The Bragg peak intensity vanishes just below the roughening transition temperature, T_R, as $\exp[-\text{constant} \times (T_R - T)^{-1/2}]$, where the constant depends on the particular Bragg peak.

1. Introduction

Atomic beam diffraction experiments have recently been carried out (Lapujoulade *et al* 1983 and references therein) on $(1, 1, 2n+1)$ faces of copper ($n = 1, 2, 3$). The Bragg peak intensity is described by a Debye–Waller factor for temperatures below $T_n \approx 400$ K, then falls off fairly abruptly. At 600 K the intensity is reduced by a factor two. In the present paper, this effect will be interpreted in terms of a roughening transition (Burton and Cabrera 1949, Weeks 1980).

The roughening transition of stepped and isotropic surfaces has been discussed recently by Tommei *et al* (1983), Schulz (1984), Bol'shov *et al* (1984), Blatter (1984) and Levi (1984). The present work, initiated before we had knowledge of these articles, contains new results summarised in § 11.

In § 2 the structure of the surface above and below the roughening transition temperature T_R is described. A simple theory of atomic beam diffraction is outlined in § 3. A dynamical, microscopic model which depends on two parameters is introduced in §§ 4 and 5. Its low-temperature behaviour is studied in § 6. In § 7 T_R and T_n are evaluated approximately. Formulae for the Landau free-energy functional are given in § 8 and the lineshape is deduced in § 9. The results are compared qualitatively with experiment in § 10.

The unit of energy is the kelvin, so that the Boltzmann constant is 1. The unit of length is generally chosen to be $a/\sqrt{2}$, where a is the side of the cubic cell.

0305-4608/85/040809 + 26 $02.25

2. Structure of the (1, 1, 2n + 1) faces of face-centred cubic metals

The structure of these faces is illustrated in figure 1, which shows the body-centred tetragonal cell of sides $(a/\sqrt{2}, a/\sqrt{2}, a)$. The (1, 1, 2n + 1) face is built of narrow strips of orientation (111) and height $a/2$, separated by broad strips of orientation (001) and width $na/\sqrt{2}$. The narrow (111) strips will hereafter be called steps. (1, 1, 2n′) faces have not been observed, to our knowledge, for $n' \neq 0$. The reason is geometrical, namely the (001) strips can only have width $na/\sqrt{2}$, with n as an integer.

The structure described above may be expected to become unstable at high temperature for large n since the steps become fuzzy, as shown in figure 2(*b*). This is the so called roughening transition described, for example, by Weeks (1980). When the steps are fuzzy, the surface is called rough. The low-temperature phase, when the steps are straight, is called smooth (figure 2(*a*)). For a more precise definition it is convenient to consider the equation $z = f(\boldsymbol{R})$ of the surface in a coordinate frame such that the z axis is along (1, 1, 2n + 1), i.e. perpendicular to the average surface direction. $\boldsymbol{R}$ is a point of a fixed (1, 1, 2n + 1) plane. The surface is called rough if the thermal average

$$\Gamma(\boldsymbol{R}) = \langle (z(\boldsymbol{R} + \boldsymbol{R}') - z(\boldsymbol{R}'))^2 \rangle \tag{1}$$

goes to infinity with $|\boldsymbol{R}|$.

There is some experimental evidence that roughening actually occurs for (113), (115), . . . , faces. A first argument is that surface defects created by irradiation may be healed by annealing. Another piece of evidence is provided by low-energy atomic beam spectroscopy, which will be described below.

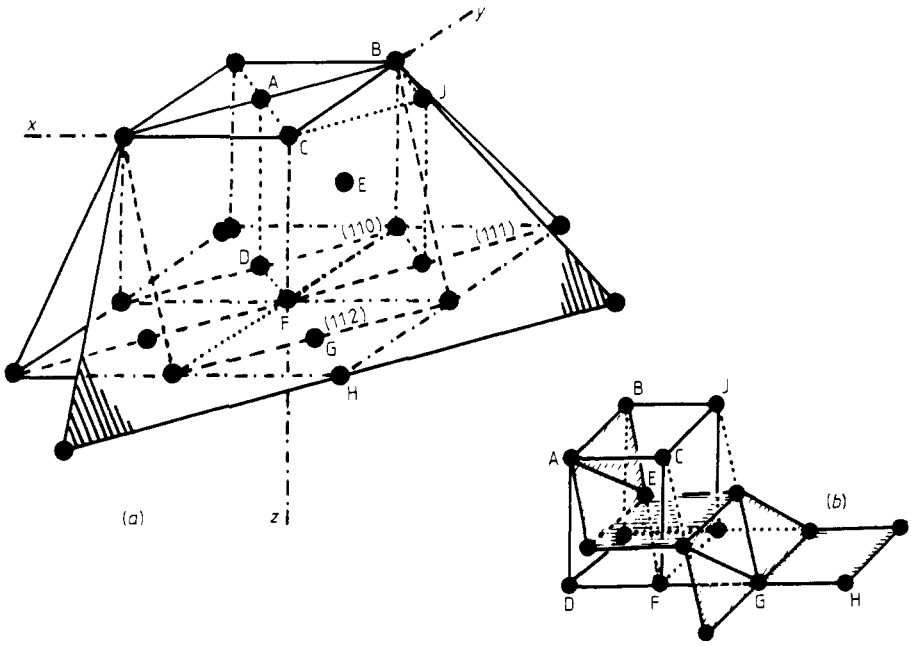

Figure 1. (*a*) The (110), (111), (112) and (113) faces of the FCC lattice. (*b*) The (113) face relative to the centred tetragonal lattice with details of the step structure.

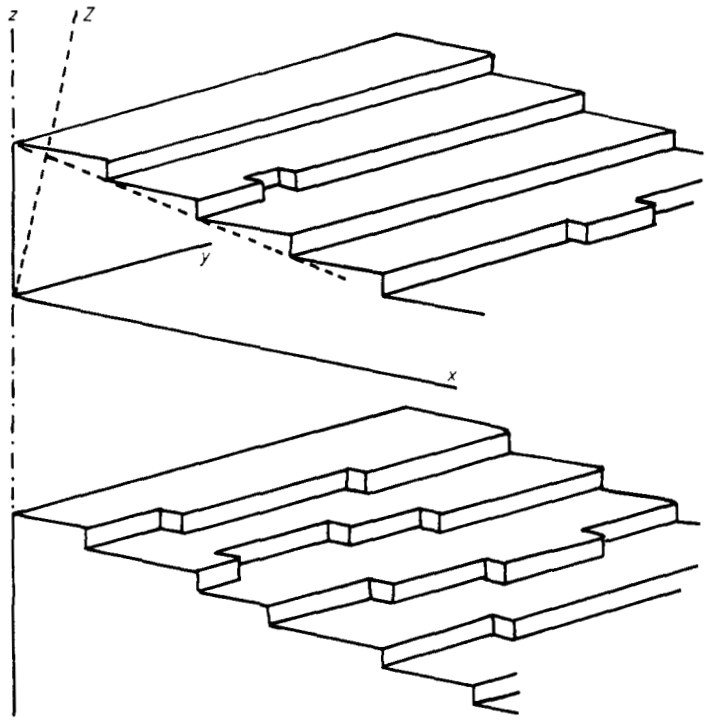

Figure 2. Schematic representation of a $(1, 1, 2n+1)$ face (a) below the roughening transition temperature T_R and (b) above T_R. The x, y, z axes are respectively the (110), (1$\bar{1}$0) and (001) directions.

3. Atomic beam diffraction

The theory of atomic beam diffraction by surfaces relies essentially on the solution of a Schrödinger equation which is time dependent because of thermal vibrations. The literature about this subject (Zaremba and Kohn 1976, Levi and Suhl 1979, Lapujoulade 1981, Garcia *et al* 1982, Armand and Manson 1979, Gorse *et al* 1984) is not particularly simple. In order to bypass the necessary complications, a simple-minded heuristic description will be given here for the use of non-specialists. Firstly, atomic motion will be neglected so that the Schrödinger equation to be solved becomes time independent. This will be called the static approximation.

Secondly, following Garcia *et al* (1979) and Lapujoulade (1981), the actual surface potential will be replaced by a 'hard-wall' potential, which is exactly zero above some equipotential surface (Σ) and infinite below (figure 3). (Σ) will hereafter be called the 'reflection surface'. Since it is an equipotential it is roughly parallel to the actual surface but, in the case of low-energy atoms, it is flatter (Gorse *et al* 1984) and does not show any strong modulation due to atomic structure.

As a last approximation, the reflected wave $\psi'(\boldsymbol{\rho})$ resulting from an ingoing plane wave $\psi_0(\boldsymbol{\rho}) = \exp(i\boldsymbol{k}_0 \cdot \boldsymbol{\rho})$ will be assumed to have the form

$$\psi'(\boldsymbol{\rho}) = -\int_{(\Sigma)} (2\pi)^{-1}\, d^2R \exp(i\boldsymbol{k}_0 \cdot \boldsymbol{R}) k_0^z \frac{\exp(ik|\boldsymbol{\rho}-\boldsymbol{R}|)}{|\boldsymbol{\rho}-\boldsymbol{R}|} \tag{2}$$

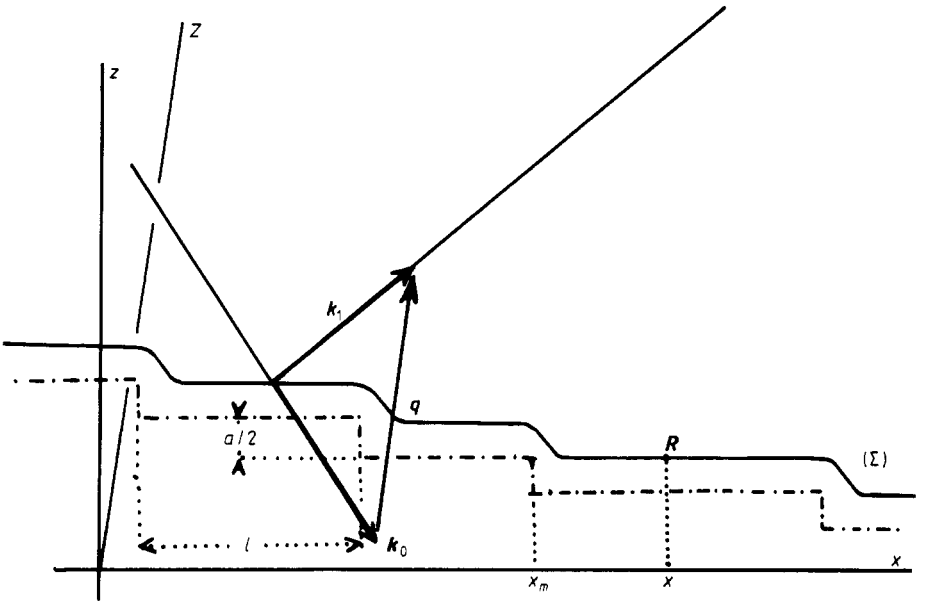

Figure 3. Section showing the reflection surface (Σ) above T_R, the incoming and outgoing wavevectors $\boldsymbol{k}_0$, $\boldsymbol{k}_1$ and the reflection vector $\boldsymbol{q}$. The chain line is a schematic representation of the actual surface.

where $k = |\boldsymbol{k}_0|$ and k_0^z is the component of $\boldsymbol{k}_0$ normal to the surface. In principle k_0^z depends on $\boldsymbol{R}$, but in practice it will be replaced by the component normal to the (001) plane, as is correct if n is large. Apart from this additional simplification formula (2) can be deduced from the Helmholz theorem and the Kirchhoff approximation (Hill and Celli 1978). Formula (2) is essentially the Huygens principle and is closely related to the so called 'eikonal' approximation (Garibaldi *et al* 1975).

The approximations introduced in this section are expected to give a qualitative but simple description of interference effects between the waves scattered by various points of the surface. The static approximation does not describe thermal motion correctly, but thermal motion is a well understood problem which is outside the scope of our investigation. The present work aims to describe fluctuations of the type displayed by figure 2(*b*). These fluctuations should be slow because they involve mass transfer. Thus, the static approximation is justified for a qualitative study of the roughening transition.

The hard-wall approximation describes qualitatively the fact that low-energy atoms (in contrast to those used for channelling) do not come into the material, and even stop at a few angstroms of the actual surface (Gorse *et al* 1984). This would be correct for atoms of wavelength $2\pi/k$ much larger than 1 Å.

Finally, the Huygens formula (2) is essentially a heuristic approximation. Similar results might be obtained from the slightly more elaborate formulae used by Hill and Celli (1978), Levi *et al* (1981, 1982), Tommei *et al* (1983) and Blatter (1984). The validity of these approximations is discussed carefully by Hill and Celli (1978).

It is convenient to choose the z axis parallel to (001), the y axis along $(1\bar{1}0)$ and the x axis along (110). Let $x_m(y)$ be the position of the mth step at ordinate y. At $T=0$ we have

$x_m = ml$ where, for a (1, 1, 2n + 1) face,

$$l = (n + \tfrac{1}{2})a/\sqrt{2} = n + \tfrac{1}{2}. \tag{3}$$

The intensity reflected in a direction $\boldsymbol{k}_1 = \boldsymbol{k}_0 + \boldsymbol{q}$ is given approximately by

$$I = 2[(1 - \cos(q_z a/2))/q_x^2 l]$$
$$\times \sum_m \int \mathrm{d}y \exp[\mathrm{i}q_y y + \mathrm{i}m(q_x l + q_z a/2)]\langle \exp[\mathrm{i}q_x(u_m(y) - u_0(0))]\rangle. \tag{4}$$

This formula is derived in appendix 1 from the Huygens approximation (2). An analogous formula has been obtained by Levi *et al* (1982). It is convenient to introduce the notation I' defined by

$$I = 2[(1 - \cos(q_z a/2))/q_x^2 l]I'. \tag{5}$$

The average value of the exponential in (4) is not easily evaluated. To simplify the calculation, the probability P_n that $(u_m(y) - u_0(0))$ has the (integral) value n will be assumed to be gaussian, $P_n = C\exp(-\alpha n^2)$, where α depends on m and y. This assumption can be justified for long distances and $T \neq T_R$, as will be seen in § 8. It is also correct for low temperatures because, as will be seen in § 6, all the P_n are negligible except $P_0 \simeq 1$ and $P_1 = P_{-1}$. This distribution is well approximated by a gaussian, with $\alpha = -\ln P_1$. Assuming a gaussian distribution and using the Poisson formula one obtains

$$\langle \exp[\mathrm{i}q_x(u_m(y) - u_0(0))]\rangle = C \sum_n \exp(-\alpha n^2 + \mathrm{i}q_x n)$$
$$= C \sum_p \int_{-\infty}^{\infty} \mathrm{d}x \exp(-\alpha x^2 + \mathrm{i}q_x x + 2\mathrm{i}\pi p x)$$
$$= C(\pi/\alpha)^{1/2} \sum_{p=-\infty}^{\infty} \exp[-(q_x + 2\pi p)^2/2\alpha].$$

For small values of α only one term of this sum is important near integral values of $q_x/2\pi$, and the whole sum is negligible for other values of q_x. A good approximation is therefore

$$\langle \exp[\mathrm{i}q_x(u_m(y) - u_0(0))]\rangle = \exp(\langle -(u_m(y) - u_0(0))^2(1 - \cos q_x)\rangle).$$

This formula is also satisfactory for large α as can be seen directly from (4), taking into account the fact that $(u_m(y) - u_0(0))$ can only be equal to 0 or ± 1 with an appreciable probability (see § 6). For intermediate values of α the above formula is an acceptable and simple approximation. Insertion into (4) and (5) yields

$$I' = \sum_m \int \mathrm{d}y \exp[\mathrm{i}q_y y + \mathrm{i}m(q_x l - q_z a/2) - \langle (u_m(y) - u_0(0))^2\rangle(1 - \cos q_x)]. \tag{6}$$

In practice the incident beam is not strictly parallel nor monochromatic, and the detector is not ideal either, so that interference effects cannot be observed between points $\boldsymbol{R}, \boldsymbol{R}'$ at a distance larger than some coherence length R_c. Mathematically, the intensity observed is the convolution of (3) with a 'resolution function' of $\boldsymbol{q}$, which may be assumed to be a gaussian of width $1/R_c$, the Fourier transform of which is

$$\Gamma(\boldsymbol{R} - \boldsymbol{R}') = (1/R_c)\exp[-(\boldsymbol{R} - \boldsymbol{R}')^2/R_c^2]. \tag{7}$$

The function $I'(q)$ defined by (6) contains a part which is the sum of two-dimensional delta functions or 'Bragg peaks':

$$I'_{\text{Bragg}} = N_n \delta_{0,q_y} \sum_p \delta_{2\pi p, q_x l - q_z a/2} \exp[-2\langle u_m^2(y)\rangle(1-\cos q_x)] \tag{8}$$

where N_n is the number of atoms per step multiplied by the number of steps and q_z is determined by the condition $(\boldsymbol{k}_0 + \boldsymbol{q})^2 = k^2$. The exponential factor in (8) is something like the Debye–Waller factor of the system of steps. It is a periodic function of q_x because $u_m(y)$ is an integer. The true Debye–Waller factor does not appear in (8) because phonons have not been taken into account.

4. Dynamical model

As can be seen from figure 2 the surface is a succession of steps and each step exhibits kinks. In order to give a statistical-mechanical analysis of the problem it is necessary to know the energy of any configuration. This energy will be assumed to be

$$W = W_0 \times \text{number of kinks} + \text{interaction between different steps.} \tag{9}$$

The second term will be discussed in the next section. It must be weak because of the large distance between steps. The energy W_0 of a kink is related to the binding energy of Cu, which will be evaluated later on to be between 0.2 and 0.3 eV. The model (9) implies several assumptions. Firstly, the number of steps is assumed to be constant, in agreement with the experimental fact that $(1, 1, 2n+1)$ faces are stable. Thus, a constant term proportional to the number of steps has been neglected in (9). Secondly, the total number of atoms on the surface is allowed to fluctuate slightly although it is actually fixed. In the limit of large size the fluctuation is weak and the procedure is expected to be correct. It is equivalent to assuming that the number of atoms may vary but that an appropriate chemical potential compensates the energy gain or energy loss when an atom sticks at the surface *at a kink*, or leaves it.

Another approximation is to neglect the interaction between kinks on the same step. This is quite justified because the kink energy W_0 is much larger than the temperatures of interest, between 100 and 700 K (Lapujoulade *et al* 1983).

Finally, the steps will always be assumed to proceed forward in the y direction (except at kinks) and never to come backward. This is probably a very good approximation.

5. Interactions between walls

The interaction between two pieces of steps at a distance r apart is analogous to the interaction between two adatoms on a surface (Desjonquères 1976, 1980). There is a repulsion proportional to $1/r^3$ due to the elastic strain produced by the steps (Lau and Kohn 1977, Gordon and Villain 1979†). There is also an electrostatic interaction energy between the electric dipoles which form on the steps. This energy is also proportional to $1/r^3$, but it is not necessarily repulsive because there is no obvious symmetry relation which obliges the dipoles to be normal to the surface. Another long-range interaction may be related to Friedel oscillations and is more complicated. As a working hypothesis, a $1/r^3$

† This Letter contains a mathematical mistake. The interaction between steps is actually always repulsive.

repulsion will be assumed between two pieces of steps at distance r. Therefore, the repulsive energy between two steps is proportional to l^{-2}. The necessary energy per atom to move one step by an interatomic distance is therefore, at $T=0$,

$$w_n = Q[1/(l-1)^2 + 1/(l+1)^2 - 2/l^2] \approx Q/l^4 = Q/(n+1/2)^4 \tag{10}$$

where Q is a constant.

Long-range repulsion between steps is necessary to ensure the stability of the low-temperature phase. With short-range interactions the surface would be rough at all temperatures, as in similar problems considered by Villain and Bak (1981), Pokrovskii and Talapov (1980) and Haldane and Villain (1981). With attractive interactions the surface would be unstable. Oscillatory interactions proportional to $1/r^2$ are predicted theoretically in certain cases (Lau and Kohn 1978) but are hardly consistent with the experimental observation of a series of $(1, 1, 2n+1)$ faces.

Also, long-range repulsion together with matter conservation account for the metastability of high-index faces. Suppression of the highest terrace in figure 2 would probably lower the energy, but matter should flow to lower terraces. This is excluded by long-range repulsion.

In this paper the temperature is always assumed to satisfy the following condition, actually fulfilled in experiments by Lapujoulade *et al* (1983):

$$w_n \ll T \ll W_0. \tag{11}$$

6. Statistical mechanics at low temperatures $T \ll T_R$

The low-temperature expansion may be calculated by the same methods as for the Ising model (Domb 1974). Only the lowest order will be calculated here.

For low temperatures the displacement $u_m(y)$ is zero for almost all values of m and y. At some places, $u_m(y) = \pm 1$, but then there is a low probability that $u_{m+1}(y)$ and $u_{m-1}(y)$ are non-zero. The probability that $|u_m(y)|$ is 2 or larger will also be neglected. The energy of a detour of p atoms starting from a given point y, on the mth step is, according to (9) and (10), $2W_0 + |y_2 - y_1| w_n$ and the probability is

$$P(m, y_1, y_2) \simeq 2 \exp(-2\beta W_0 - \beta w_n |y_2 - y_1|) \tag{12}$$

where the factor 2 accounts for the fact that the detour may be to the right or to the left.

The average value $\langle u_m(y') u_{m'}(y'+y) \rangle$ $(y \geqslant 0)$ vanishes for $m' \neq m$ as a consequence of the approximations made. For $m' = m$, one should sum (12) over all values of y_1 and y_2 which satisfy the conditions $y_1 < y' \leqslant y' + y < y_2$. Note that if y_1 is an integer, y' and $(y'+y)$ are half integers because the centres of the atoms are at y_1, while y' lies between two atoms. We find that

$$\langle u_m(y') u_m(y'+y) \rangle \simeq 2 \exp[-2\beta W_0 - \beta w_n(|y|+1)] \left(\sum_{q=0}^{\infty} \exp(-\beta q w_n) \right)^2$$

or, according to (11),

$$\langle u_m(y') u_{m'}(y'+y) \rangle \simeq 2(T/w_n)^2 \exp(-2\beta W_0) \exp(-\beta w_n |y|) \delta_{mm'}. \tag{13}$$

It is of interest to introduce the Fourier transform

$$u_q = (1/\sqrt{N_n}) \sum_{m,y} u_m(y) \exp(\mathrm{i}\tilde{q}_x m + \mathrm{i} q_y y) \tag{14}$$

where N_n is the number of degrees of freedom of the system of steps (see § 3) and

$$\tilde{q}_x = q_x l. \tag{15}$$

From (13), (11) and (14) we deduce that

$$\langle |u_q|^2 \rangle \simeq 2a^2(T/w_n)[\exp(-2\beta W_0)/(\beta^2 w_n^2 + 4\sin^2(q_y a/2\sqrt{2}))] \tag{16}$$

where the lattice constant a has been re-introduced.

Step roughness may be neglected when (13) is very small for all values of y, in particular for $y=0$. This happens for temperatures T lower than a temperature T_n defined by

$$(w_n/T_n)\exp(W_0/T_n) = C \tag{17}$$

where C is a constant of order unity. Formula (17) was obtained by Lyuksyutov *et al* (1981) and Pokrovskii and Talapov (1984) in relation to an adsorption problem.

T_n is easily deduced from Lapujoulade *et al* (1983). It is the temperature at which experimental points deviate from the 'theoretical' curve, which is essentially the Debye–Waller factor derived from the usual phonon theory (Armand and Manson 1979, Levi and Suhl 1979, Mayer 1981). For instance, for the (113) face figure 5 of Lapujoulade *et al* indicates $T_n \simeq 500$ K. Relations (10) and (17) yield

$$(T_{n'}/T_n)\exp(W_0/T_n - W_0/T_{n'}) = (l/l')^4 = [(2n+1)/2n'+1)]^4. \tag{18}$$

Experimentally, T_n does not depend very strongly on n. This indicates a high value of W_0. However, experimental data for the (113), (115) and (117) faces are consistent with (18).

The temperature T_n given by (17) is not the roughening transition temperature T_R. However, it will be seen in § 7 that T_R is of the same order of magnitude (see equation (30)).

6.1. *Value of* W_0

Assuming pair interactions, W_0 can be deduced from the cohesive energy of Cu which is 3.5 eV per atom or 3.5/6 eV per pair. We can create two kinks on a step by breaking one bond. Therefore

$$W_0 = 3.5/12 \text{ eV} = 3400 \text{ K}.$$

Another approximate evaluation is the following, which takes band effects into account. The bandwidth is proportional to the square root of the second moment, which is proportional to z, the number of neighbours. Assuming a constant distance between neighbours, the energy is $3.5 \text{ eV} \times \sqrt{7/12}$ for an atom on a step, and $3.5 \text{ eV} \times \sqrt{6/12}$ for an atom on a kink of a step. Hence $W_0 = 3.5 \text{ eV} \times (\sqrt{7}-\sqrt{6})/\sqrt{12}$ or $W_0 \approx 0.2 \text{ eV} = 2300 \text{ K}$.

6.2. *Reflected intensity*

Insertion of (13) into (6) yields

$$I' = I'_{\text{Bragg}} + (8T/w_n)[\exp(-2\beta W_0)/(\beta^2 w_n^2 + q_y^2)]$$
$$\times (1-\cos q_x)\exp[-2\langle u_m^2(y)\rangle(1-\cos q_x)] \tag{19}$$

where the exponential of the small quantity $\langle u_m(y)u_0(0)\rangle$ has been expanded. The first term

of (19) is given by (8). The second term is completely diffuse in the x direction but sharply peaked around $q_y = 0$. In the present approximation the satellites at $q_y = 2n\pi$ vanish. This is not completely true because the scattering surface is slightly modulated by the atomic structure.

7. Exactly solvable models and roughening temperature

In order to study the situation at higher temperatures the model should be more completely defined. The Hamiltonian is expected to have the form

$$\mathscr{H} = \sum_{m,y} W_0(u_m(y+1) - u_m(y))^2 + \sum_{m,m'} \sum_{y,y'} f(m'-m, y'-y; u_{m'}(y') - u_m(y)) \tag{20a}$$

with the conditions

$$u_m(y) = \text{integer} \tag{20b}$$

$$u_{m+1}(y) - u_m(y) > -l. \tag{20c}$$

The detailed form of the function f might in principle be known for large distances from elasticity theory and electrostatics, but no attempt will be made to realise this ambitious programme. By means of appropriate approximations, the problem will be defined in terms of the parameters W_0 and w_n defined in §§ 4 and 5.

Firstly, an argument similar to that of § 5 suggests that f decreases as $(m'-m)^{-5}$ or $(m1-m)^{-4}$ after integration over y. This decrease is sufficiently rapid so that we can keep only interactions between nearest neighbours, $m'-m=1$. This point will be discussed further in § 8.

Secondly, condition (11) implies that walls are constituted of long straight lines, so that $u_{m+1}(y') = u_{m+1}(y)$ in the whole range where f is appreciable. Formula (20a) now reads

$$\mathscr{H} = W_0 \sum_{m,y} (u_m(y+1) - u_m(y))^2 + \sum_{m,y} g(u_{m+1}(y) - u_m(y)) \tag{21}$$

where, according to § 5,

$$g(u) = Q(l+u)^{-2}. \tag{22}$$

A model which is exactly soivable is obtained if (22) is replaced by the approximations

$$g(u) = 0 \qquad u \geqslant 0 \tag{23a}$$

$$g(-1) = w_n \tag{23b}$$

$$g(u) = \infty \qquad u < -1. \tag{23c}$$

The problem can be treated by the transfer matrix method. Let N_s be the number of steps. The obvious relations $u_1(y) > -l$ and $u_{N_s}(y) < l$, together with (23c), imply that

$$-l - m < u_m(y) < l + N_s - m \tag{24}$$

where the additive constants $\pm l$ may be neglected for a large sample. A consequence of (24) is that the quantities

$$v_m(y) = 2m + u_m(y) \tag{25}$$

satisfy the relations

$$0 < v_1(y) < v_2(y) < \ldots < v_{N_s}(y) \leqslant 2N_s. \tag{26}$$

It is convenient to introduce a variable $v = 1, 2, 3, \ldots, 2N_s$ and a spin $\sigma_v^z(y)$ defined by

$$\sigma_v^z(y) = \tfrac{1}{2} \qquad \text{if } v = v_m(y) \text{ for some } m$$

$$\sigma_v^z(y) = -\tfrac{1}{2} \qquad \text{otherwise.}$$

The Hamiltonian defined by (21) and (23) can easily be expressed in terms of the σ_v^z. We then introduce the transfer operator. The non-commutativity of its various parts may be neglected if relation (11) is satisfied, and the transfer operator is then easily seen to be the exponential of the Hamiltonian of a spin-$\frac{1}{2}$ Heisenberg–Ising antiferromagnetic linear chain:

$$\hat{H} = -\sum_v (\sigma_v^x \sigma_{v+1}^x + \sigma_v^y \sigma_{v+1}^y + B\sigma_v^z \sigma_{v+1}^z) \tag{27}$$

where the v are integers and

$$B = (w_n/2T) \exp(W_0/T), \tag{28}$$

and then Hamiltonian (23) follows. An important point is that (26) implies

$$\sum_{v=1}^{2N_s} \sigma_v^z = 0. \tag{29}$$

If this condition is not satisfied, there is no roughening transition (Haldane 1980). This means that if the surface has a few extra steps it is rough at all temperatures. This result is a consequence of the approximation (23*a*).

In the absence of a magnetic field (27) shows a phase transition at $B = 1$. For $B > 1$ there is long-range antiferromagnetic order along the z direction and a gap in the excitation spectrum. In terms of the original model this corresponds to well defined steps and terraces and a finite correlation length for fluctuations. At the transition point the gap vanishes and the system remains gapless for all $B < 1$. In this region the spin system exhibits XY-like behaviour with no long-range order or power-law decay of correlations. This phase corresponds to the rough phase of the crystal face. From (28) we locate the transition temperature

$$(W_n/T_R) \exp(W_0/T_R) = 2. \tag{30}$$

This relation is analogous to (17) and shows that T_R and T_n are of the same order of magnitude. The transition is of infinite order (Baxter 1982) and is in the Kosterlitz–Thouless universality class. In the ordered phase, near $B = 1$, the gap vanishes as

$$\Delta \sim \exp\{-\tfrac{1}{2}\pi^2/[2(B-1)]^{1/2}\} \tag{31}$$

(Baxter 1982). This implies that in the original model the correlation length ξ diverges as

$$\xi \sim \exp(\text{constant}/\sqrt{T_R - T}). \tag{32}$$

The specific heat and order parameter show similar singularities.

Another solvable model, closely related to the present one, has recently been introduced by Abraham (1983). The model uses a condition similar to (22) but otherwise can be solved exactly. The solution is based on the fact that the allowed wall configurations can be put into correspondence with those of the six-vertex model in an electric field, and proceeds by application of the Bethe ansatz. Since the Heisenberg–Ising chain (27) is itself equivalent to the six-vertex model (Baxter 1982) it follows that Abraham's and the present model exhibit the same phase transitions and identical critical behaviour.

It should be noticed that although these exactly solvable models confirm the existence of the phase transition and give the exact nature of the singularities in the thermodynamic functions, they are of little use for the calculations of the correlation functions. Indeed, the correlation function required, $\langle \exp[ik(u_m(y)-u_m(0))]\rangle$, cannot be expressed solely in terms of the spin correlation function of the Heisenberg–Ising chain although, of course, its long-distance behaviour is closely related to that of the latter. For this reason we turn to a more intuitive method that captures the essence of the exact solutions as far as the critical behaviour is concerned and leads also to a calculation of the correlation functions.

8. Free-energy functional

As seen from (6), we need the correlation function $\langle (u_m(y)-u_0(0))^2\rangle$. This information is not easy to obtain from the Bethe ansatz methods of § 7. Furthermore, the long-range character of the interaction between steps, pointed out in § 5, is offset by the approximation (23*a*) and it is of interest to check whether it is correct. For these reasons, another approach will be used from now on, namely length rescaling.

In contrast with the Bethe ansatz, rescaling methods are extremely physical and intuitive. The general idea is to evaluate thte free-energy functional $\mathscr{F}$ as a function of the long-wavelength Fourier components

$$\tilde{u}_m(y)=(1/\sqrt{N_l})\sum_{\substack{\tilde{q}_x<q_{cx}\\ q_y<q_{cy}}} u_q \exp(i\tilde{q}_x m + iq_y y) \tag{33}$$

where q_{cx} and q_{cy} are appropriate cut-offs. $\mathscr{F}$ is defined by the fact that the probability of a given distribution $\{u_q\}$ is proportional to $\exp[-\beta\mathscr{F}(\{u_q\})]$. The simplest form of the free energy $\mathscr{F}$ which can describe the qualitative features of the present model was introduced by José *et al* (1977), namely

$$\mathscr{F}=\tfrac{1}{2}\sum_q (\eta q_y^2+\eta'\tilde{q}_x^2)|u_q|^2 + U\sum_{my}(1-\cos 2\pi\tilde{u}_m(y)). \tag{34}$$

The last term favours values of u_m which are close to integers, and is a consequence of (20*b*). The first term implies a harmonic approximation of the second term of (20*a*). Neglecting possible renormalisation of η', we obtain

$$\eta'=\sum_{m,y} m^2 f''(m,y;0) \tag{35}$$

where $f''(m,y;z)$ denotes the second derivative with respect to z. This quantity can also be identified with w_n, as seen by moving a single step by ± 1:

$$\eta'=w_n. \tag{36}$$

The harmonic approximation in the first term of (34) overestimates the interaction between steps for large $(u_{m+1}-u_m)$, in contrast with (23*a*), and underestimates the interaction for negative values, in contrast with (23*c*). For large n, the harmonic approximation is better, but not necessarily in the cases which have been studied experimentally. Anyway, both models are in qualitative agreement and predict a roughening transition at a temperature given approximately by (17), as will be seen.

Before starting the rescaling procedure, $\tilde{u}_m(y)=u_m(y)$, $q_{cx}=q_{cy}=2\pi$, formula (20*b*) implies $U=\infty$. The free energy (34) should be identical to the Hamiltonian (20*a*) apart from a long-wavelength approximation $(1-\cos q_y \sim \frac{1}{2}q_y^2,\ 1-\cos\tilde{q}_x \simeq \frac{1}{2}\tilde{q}_x^2)$ which actually

is not strictly necessary. This implies $\eta = W_0$. It may be of interest to notice that, if f is replaced by a quadratic form, if condition (20*c*) is released, if $u_{m'}(y')$ is replaced by $u_{m'}(y)$ *and* if interactions beyond nearest neighbours ($|m'-m|>1$) are neglected, the Hamiltonian (20*a*) reduces to the sos model studied by Chui and Weeks (1976):

$$\mathscr{H} = W_0 \sum_{m,y} (u_m(y+1) - u_m(y))^2 + w_n \sum_{m,y} (u_{m+1}(y) - u_m(y))^2. \tag{37}$$

This model is known to have a roughening transition. It can be transformed into a two-dimensional Coulomb gas (Chui and Weeks 1976) which can then be transformed into the 'sine–Gordon' model (34). However, the usual derivation involves certain approximations which are not good in the anisotropic situation considered here, $W_0 \gg w_n$. But the transformation of (37) into (34) can be achieved by length rescaling, as seen in appendix 2.

The transformation of the free energy (34) under length rescaling has been studied by many authors (José *et al* 1977, Wiegmann 1978, Ohta and Kawasaki 1978, Ohta 1978, Amit *et al* 1980, Knops and Den Ouden 1980). They have shown that there is a roughening transition at a temperature T_R which is given, if U is small, by the relation $\sqrt{\eta\eta'} = \frac{1}{2}\pi T$. Using the value of η calculated in appendix 2 (see also table 1 below), we find that

$$(w_n/T_R)\exp(W_0/T_R) = \tfrac{1}{2}\pi^2. \tag{38}$$

This value is more than twice as large as (30) but, as seen in appendix 3, there is a large correction due to the finite value of U which reduces the right-hand side of (38). There is no doubt about the existence of a phase transition because we have a good theory at high temperature which predicts a rough phase, and a good theory at low temperature which predicts straight, well ordered steps. When q_{cx} and q_{cy} are decreased, the parameter U of formula (34) goes to a limit U_∞. The definition of the roughening transition implies $U_\infty = 0$ for $T > T_R$ and $U_\infty \neq 0$ below T_R. Replacing the cosine in (34) by its second-order Taylor expansion, we obtain a harmonic free energy which easily yields the average values:

$$\langle |u_q|^2 \rangle = T/(\eta q_y^2 + \eta' \tilde{q}_x^2 + 4\pi^2 U_\infty). \tag{39}$$

Comparison with (17) gives, for $T \ll T_R$,

$$\eta = \tfrac{1}{4} w_n \, \mathrm{e}^{2\beta W_0} \tag{40}$$

and

$$U_\infty = (\beta^2 w_n^3/8\pi^2)\, \mathrm{e}^{2\beta W_0}. \tag{41}$$

Formula (39) holds for small q, at $T \neq T_R$. The values of η and η' for small q are renormalised and differ somewhat from the values (36) and (A.9). In terms of these

Table 1. Parameter values above and below T_R.

	$T < T_R$	$T > T_R$
$\sqrt{\eta\eta'}/T$	$> \frac{1}{2}\pi$	$< \frac{1}{2}\pi$
η	$\frac{1}{4} w_n \, \mathrm{e}^{2\beta W_0}$	$\frac{1}{2} T \, \mathrm{e}^{\beta W_0}$
η'	w_n	w_n
U_∞	$(\beta^2 w^3/8\pi^2)\, \mathrm{e}^{2\beta W_0}$ (for $T \ll T_R$ only)	0
$\langle \lvert u_q \rvert^2 \rangle$	$T[\eta q_y^2 + \eta'(n+\frac{1}{2})^2 q_x^2 + 8\pi^2 U_\infty/a^2]^{-1}$	

renormalised parameters the following relation (Ohta 1978, José *et al* 1977) is exact:

$$\sqrt{\eta\eta'}|_{T=T_R} = \tfrac{1}{2}\pi T_R. \tag{42}$$

The values of the relevant parameters derived in this section and in appendix 2 are summarised in table 1.

One advantage of the present approach compared with that of § 7 is that the long-range nature of the interaction may be taken into account. According to § 5, the function f'' in (35) should be proportional to $(m^2l^2 + y^2)^{-5/2}$. The result of the summation on y is proportional to m^{-4}. This ensures the convergence of the sum (35). If the interactions between steps were proportional to $1/m$ or larger, the surface would never become rough.

9. Fluctuations

In expression (6) which describes atom diffraction spectra, the quantity to be evaluated is

$$\langle (u_m(y) - u_0(0))^2 \rangle = (2/N) \sum_{\tilde{q}_x q_y} \langle |u_q|^2 \rangle (1 - \exp[i(\tilde{q}_x m + q_y y)]).$$

The average value is given by (39) with a good approximation at long distances for $T \neq T_R$.

For $T \geqslant R_R$ we find from appendix 3 (formula (A.48))

$$\Gamma(\rho) \equiv \langle (u_m(y) - u_0(0))^2 \rangle = (T/\pi\sqrt{\eta\eta'}) \int_0^{p_1} (\mathrm{d}p/p)(1 - J_0(p\rho)) \tag{43}$$

where p_1 is a cut-off and

$$\rho = [y^2(\eta'/\eta)^{1/2} + m^2(\eta/\eta')^{1/2}]^{1/2}.$$

Relation (43) gives

$$\frac{\partial\Gamma(\rho)}{\partial\rho} \simeq \frac{T}{\pi\sqrt{\eta\eta'}} \frac{1}{\rho} \tag{44}$$

whence

$$\Gamma(\rho) = \text{constant} + (T/\pi\sqrt{\eta\eta'}) \ln \rho \tag{45}$$

where the constant depends upon the short-wavelength degrees of freedom.

At T_R we find (see appendix 3)

$$\Gamma(\rho, T = T_R) = \text{constant} + (2/\pi^2) \ln \rho, \tag{46}$$

a universal behaviour.

For $T > T_R$ the Debye–Waller exponential in (8) vanishes and, if the diffraction pattern is interpreted in terms of delta functions, its intensity is zero. However, it is probably possible to interpret directly the lineshape observed experimentally with the help of (6), (44) and (45). The intensity is

$$I'(q_x, q_y, q_z) = \sum_m \int \mathrm{d}y \exp[iq_y y + im(q_x l - q_z a/2)] \times (m^2\sqrt{\eta/\eta'} + y^2\sqrt{\eta'/\eta})^{-(T/\pi\sqrt{\eta\eta'})(1-\cos q_x)}. \tag{47}$$

As seen in appendix 4, this can be transformed into

$$I'(\boldsymbol{q}) = \sum_{\nu=-\infty}^{\infty} [\Gamma(2-\tau)/\Gamma(\tfrac{1}{2}\tau)\Gamma(\tfrac{3}{2} - \tfrac{1}{2}\tau)] P_\nu^{-2+\tau}(q) \tag{48}$$

where

$$P_\nu^2(\boldsymbol{q}) = \tfrac{1}{2}a^2 q_y^2 \sqrt{\eta/\eta'} + (q_x l - q_z a/2 + 2\pi\nu)^2 \sqrt{\eta'/\eta}$$

and

$$\tau(\boldsymbol{q}) = -(T/\pi\sqrt{\eta\eta'})(1 - \cos q_x). \tag{49}$$

The intensity (48) has a singularity when the following 'Bragg conditions' are satisfied: $q_y = 0$, $(q_x l - q_z a/2)/2\pi$. However, the intensity is only infinite for those Bragg positions which satisfy the additional condition $T(1 - \cos q_x) < \pi\sqrt{\eta\eta'}$.

For $T \lesssim T_R$ it is shown in appendix 3 that (43) has to be modified as follows in terms of an appropriate cut-off p_1:

$$\Gamma(\rho) = (T/\pi\sqrt{\eta\eta'}) \int_0^{p_1} [p\, \mathrm{d}p/(p^2 + \xi^{-2})](1 - J_0(p\rho)) \tag{50}$$

where the correlation length diverges near the critical point

$$\ln \xi \approx |(T - T_R)/T_R|^{-1/2} \qquad (T < T_R). \tag{51}$$

Formula (50) yields

$$\Gamma(\rho) = (2/\pi^2)(|t|^{-1/2} - K_0(\rho/\xi)) \tag{52}$$

where $|t| \propto |(T - T_R)/T_R|$ and K_0 is the Bessel function of the second kind.

By a derivation similar to the one that leads to equation (A.59) in appendix 4, the intensity below but near T_R is found to be

$$I' = \sum_{\nu=-\infty}^{\infty} I'_\nu$$

with

$$I'_\nu = 2\pi \int_0^\infty \rho J_0(p_\nu, \rho) \exp[(2q_x^2/\pi^2)(K_0(\rho/\xi) - |t|^{-1/2})]\, \mathrm{d}\rho \tag{53}$$

and p_ν is as defined above.

By dividing the range of integration into two parts, $\rho \ll \xi$ and $\rho \gg \xi$, and using the asymptotic properties of the Bessel functions, (53) can be approximately divided into two parts:

$$I'_\nu = I'_{1\nu} + I'_{2\nu}.$$

$I_{1\nu}$ leads to the usual series of Bragg peaks

$$I'_{\mathrm{Bragg}} = \sum_{\nu=-\infty}^{\infty} I'_{1\nu} = \sum_p \delta_{q_x l - q_z a/2,\, 2\pi p}(\exp[-(2q_x^2/\pi^2)|t|^{-1/2}]) \tag{54}$$

and $I'_{2\nu}$ is a background given by

$$I'_{2\nu} \approx 2\pi \int_0^\infty \exp(-\rho/\xi)\rho^{1-(2/\pi^2)q_x^2} J_0(P_\nu \rho)\, \mathrm{d}\rho. \tag{55}$$

As $|t| \to 0$ the intensity of the Bragg peaks decreases and the background term takes over. It can be easily seen that, at $|t| = 0$, (55) exactly matches formula (48) derived above T_R, as it should.

10. Comparison with experiment

The experimental data of Lapujoulade *et al* (1983) have been interpreted in terms of Bragg peaks. The typical Bragg peak intensity is displayed in figure 4. Conventionally, a Bragg peak is a delta function in the intensity as a function of the scattering vector q. Above T_R the Bragg peaks (in the conventional sense) vanish but the intensity (47) does exhibit sharp maxima at the Bragg positions, which are in practice not easily distinguished from conventional Bragg peaks. Even below T_R the 'diffuse' part (55) may be confused with conventional Bragg peaks. Thus, a detailed comparison between theory and experiment would require a careful analysis of the experimental lineshape. This analysis is not available. A more quantitative, numerical theory would also be desirable.

For these reasons we shall only consider the low-temperature region, when the intensity is given by (19). The diffuse part will be ignored and our attention will be focused on the Bragg part given by (8). The intensities observed by Lapujoulade *et al* (1983) can be expressed as

$$I_G = I_G^0 \, e^{-2W_G(T)} \gamma_G(T) \tag{56}$$

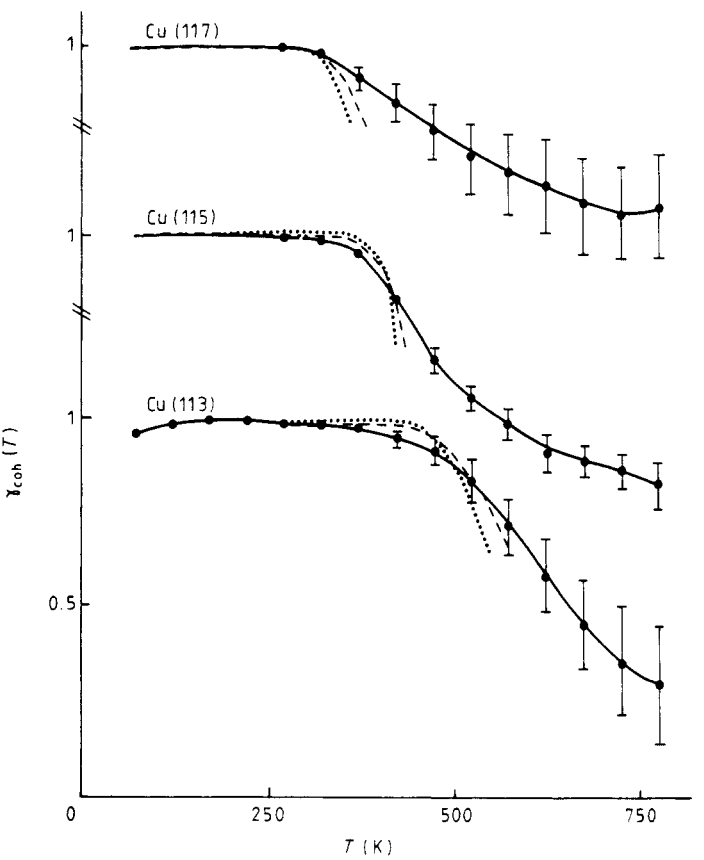

Figure 4. Intensity roughening factor $\gamma_{coh}(T)$ for the diffraction of He by Cu (113), (115), (117). ⧳, experimental data. The full curve is a guide to the eye. The dotted and broken curves are theoretical results corresponding respectively to the values $W_0 = 3400$ K and $W_0 = 2300$ K. The fitted values of w_n are given in the text.

where I_G^0 is the intensity of the Gth peak for a perfectly ordered and motionless lattice and $\boldsymbol{G}$ is a surface reciprocal lattice vector, defined by $G_x l + G_z a/2 = 0$, $G_x l - G_z a/2 = 2\pi p$, $G_y = 2\pi p'$, where p' should vanish according to (8) and is in practice very small. $2W_G(T)$ is the Debye–Waller factor due to thermal motion and $\gamma_G(T)$ is the structural roughening factor. From an extrapolation of the low-temperature data where $\gamma_G(T) \simeq 1$ it is possible to obtain $\gamma_G(T)$ from the experimental data. This has to be compared with its value calculated from (8):

$$\gamma_G(T) = 1 - 2\langle u_m^2 \rangle (1 - \cos q_G^x) \tag{57}$$

where $\boldsymbol{q}_G$ is defined by $q_G^x l - q_G^z a/2 = G_x l - G_z a/2$, $q_G^y = G_y = 0$ and $(\boldsymbol{k}_0 + \boldsymbol{q}_G)^2 = k^2$. We must emphasise once more that the roughening factor (57) has been obtained using severe approximations which are expected to be valid only when the terrace width is large with respect to the lattice parameter. This is not the case with the faces which are studied here where we have $l = 1.5$, 2.5 and 3.5, respectively. The dependence upon q_G^x displayed by (57) is expected to be especially realistic. So a comparison between (57) and the data for each diffraction peak would be very tedious and possibly meaningless. Thus we prefer to calculate, for given incidence conditions, the total coherent diffraction intensity given by

$$\gamma_{\text{coh}}(T) = \sum_G \gamma_G(T) = \frac{\Sigma_G I_G}{\Sigma_G I_G^0 \, e^{-2W_G(T)}}.$$

We then replace $\cos q_G^x$ in (57) by its average over the different peaks, i.e. $\langle \cos q_G^x \rangle = 0$, so that we get

$$\gamma_{\text{coh}}(T) \simeq 1 - 2\langle u_m^2 \rangle.$$

Figure 4 shows the experimental values of $\gamma_{\text{coh}}(T)$ for the different faces which have been studied. Before comparing these data with the model we have to make the following remarks.

(i) The error bars are not due to the experimental uncertainties but simply reflect the crudeness of the approximation $\langle \cos q_G^x \rangle = 0$.

(ii) The tendency of the curve to level out at high temperatures is due to an increase of the inelastic background which has not been subtracted. For Cu (117) this is expected to be significant immediately above the threshold temperature so that the slope of the curve is certainly greatly affected.

(iii) For Cu (117) a threshold effect at $T_n \simeq 315$ K is very clear. This is less pronounced on the other faces.

Assuming the above value for Cu (117) we get the expected T_n for the other faces from (18):

		$W_0 = 3400$ K	$W_0 = 2300$ K
Cu (115)	$T_n =$	356	371
Cu (113)	$T_n =$	431	479

Figure 4 shows that there is a slightly better agreement with $W_0 = 3400$ K. However, the other value (discussed in § 6) cannot be rejected because the threshold is not very well defined. As explained at the beginning of this section, the reason for the relatively slow

decrease of intensity with increasing temperature may be that some 'diffuse scattering' (formula (55)) has been attributed to Bragg scattering

The fit of figure 4 has been obtained with the following adjusted values of w_n (in kelvin):

Face	113	115	117
w_n (for $W_0 = 2300$ K)	32.5	8.10	3.50
w_n (for $W_0 = 3400$ K)	3.5	0.58	0.13

Relation (10) is not satisfied by the (113) face in any case, and this is not too surprising because the steps are so close to each other. In the case of the (115) and (117) faces, (10) is reasonably well satisfied provided we choose $W_0 = 3400$ K.

11. Conclusions

The basic results of this paper are the following.

(i) For temperatures lower than the roughening temperatures T_R, the reflected intensity is a sum of Bragg peaks, as seen from (8).

(ii) The Debye–Waller factor (not included in (8)) is given by the usual phonon theory below a temperature T_n. Between T_n and T_R there is an additional weakening factor displayed by (8).

(iii) T_n and T_R satisfy relation (17). Relation (18) is deduced by assuming elastic and electrostatic repulsion between steps.

(iv) The experimental data are roughly consistent with (17) and (18). The appropriate value of W_0 is consistent with the value 0.3 eV deduced from pair interactions, as well as the value 0.2 eV expected from naive band theory. The parameter Q which characterises the repulsion between steps (relation (10)) cannot be deduced from existing experiments. Relations (17) and (18) can be applied for large n only. The experimental data of Lapujoulade *et al* (1983) suggest that the (110) face also roughens at a fairly low temperature, but this is another story.

(v) Above T_R the lineshape is no longer given by (8), but by (48). The exponent τ increases rapidly with temperature according to formula (49) and table 1. This is in qualitative agreement with the experimental data of Lapujoulade *et al* (1983), although these data have been interpreted in terms of Bragg peak intensities and this is incorrect above T_R on account of (48). The vanishing of the 'Debye–Waller' factor predicted by (54) and the variation of τ with q_x^2 in the lineshape above T_R, according to (49), and in the background term below T_R, according to (55), require an experimental check.

Our results concerning the Debye–Waller factor are in disagreement with the statements of Lyuksyutov *et al* (1981) and Pokrovskii and Talapov (1984). They agree with recent work (Tommei *et al* 1983, Schulz 1984, Bol'shov *et al* 1984, Levi 1984). With respect to these papers, the present work contains some new results, for example formulae (18) and (54).

There should be some temperature above which steps do not proceed uniformly forward in the y direction. This corresponds to melting in the adsorption problem (Pokrovskii and Talapov 1984) and to the transition to paramagnetism in magnetic problems (Villain and Bak 1981). Here it corresponds to the roughening transition of the (001) face, which is found to occur experimentally at $T > 700$ K, since the intensity follows the usual Debye–Waller factor up to that temperature (Lapujoulade *et al* 1983).

Acknowledgments

It is a pleasure to thank Drs Desjonquères, Jardin and Spanjaard for illuminating discussions, and Professor Nozières for his interest in this problem.

Appendix 1. Reflection of atomic beams on a hard surface

To solve the Schrödinger equation

$$-\nabla^2\psi(\boldsymbol{\rho})+V(\boldsymbol{\rho})\psi(\boldsymbol{\rho})=-k^2\psi(\boldsymbol{\rho})$$
$$\psi(\boldsymbol{R})=0\ (\boldsymbol{R}\in\Sigma)\qquad(\text{above }(\Sigma)) \tag{A.1}$$

we make the ansatz

$$\psi(\boldsymbol{\rho})=\exp(\mathrm{i}\boldsymbol{k}_0\cdot\boldsymbol{\rho})-\int_{(\Sigma)}\mathrm{d}^2R\ G(\boldsymbol{R})\exp(\mathrm{i}\boldsymbol{k}_0\cdot\boldsymbol{R})\exp(\mathrm{i}k|\boldsymbol{R}-\boldsymbol{\rho}|)/|\boldsymbol{R}-\boldsymbol{\rho}|. \tag{A.2}$$

Above the surface (A.2) satisfies (A.1). $G(\boldsymbol{R})$ is determined by the condition $\psi(\boldsymbol{R})=0$ if $\boldsymbol{R}\in(\Sigma)$. We find for $\boldsymbol{R}\in(\Sigma)$

$$\int_{(\Sigma)}\mathrm{d}^2R'G(\boldsymbol{R}')\exp[\mathrm{i}\boldsymbol{k}_0\cdot(\boldsymbol{R}'-\boldsymbol{R})+k|\boldsymbol{R}'-\boldsymbol{R}|]/|\boldsymbol{R}'-\boldsymbol{R}|=1. \tag{A.3}$$

The solution of this equation is, basically, given by Garcia *et al* (1979). The Huygens formula (2) (used in § 2) is not equivalent to their solution even to order zero, but it is exact if (Σ) is a plane, as can be seen from (A.3).

The reflection surface (Σ) will be approximated by planar parts parallel to the (001) plane of the equation $z=0$. The planar parts are separated by steps. This picture, suggested by Gorse *et al* (1984), neglects the modulation of the scattering surface by the crystal structure. If this is correct, most of the scattering by a (001) face should be concentrated in the specular peak, which is true (Lapujoulade *et al* 1983). At $T=0$ the steps are oriented along the $(1,-1,0)$ axis since they are orthogonal to the (001) and (111) directions as seen in § 1. Let the $(1,-1,0)$ axis be denoted y and let the x axis be parallel to the (110) direction. Let $x_m(y)$ be the position of the mth step at ordinate y. The intensity reflected at large distance $\boldsymbol{\rho}=\boldsymbol{k}_1\rho/k$ of a surface of area A is proportional to Ik_0^2A/ρ^2, where I is given, according to (2), by the formula

$$AI=\int\int\int\int \mathrm{d}x\,\mathrm{d}x'\,\mathrm{d}y\,\mathrm{d}y'\exp[\mathrm{i}q_x(x-x')+\mathrm{i}q_y(y-y')]$$
$$\times\langle\exp[\mathrm{i}q_z(z(x,y)-z(x',y'))]\rangle/\cos\theta(x,y)\cos\theta(x',y') \tag{A.4}$$

where $(q_x,q_y,q_z)=\boldsymbol{q}=\boldsymbol{k}_1-\boldsymbol{k}_0$. $x, y, z(x,y)$ are the coordinates of a point $\boldsymbol{R}$ of (Σ) and $\theta(x,y)$ is the angle of (Σ) with the (001) plane at $\boldsymbol{R}$. The case of interest is that of a $(1,1,2n+1)$ face with large n, so that $\cos\theta(x,y)$ may be replaced by 1 to a reasonable approximation. If the (001) plane is decomposed into strips separated by two consecutive

steps, formula (A.4) reads

$$AI = q_x^{-2} \sum_{mm'} \int\int \mathrm{d}y\, \mathrm{d}y' \exp[\mathrm{i}q_y(y-y') - \mathrm{i}q_z(m-m')a/2] \langle (\exp(\mathrm{i}q_x x_{m+1}(y)) - \exp(\mathrm{i}q_x x_m(y))(\exp(-\mathrm{i}q_x x_{m'+1}(y')) - \exp(\mathrm{i}q_x x_{m'}(y'))) \rangle. \tag{A.5}$$

Let

$$u_m(y) = x_m(y) - ml$$

be the displacement of the mth step with respect to its position at $T=0$, which is ml, with $l=(n+\frac{1}{2})a/\sqrt{2}$. Rearranging the sum, (A.5) may be written after some calculation as

$$I = 2[(1-\cos(q_z a/2))/q_x^2 A] \sum_{mm'} \int\int \mathrm{d}y\, \mathrm{d}y' \exp[\mathrm{i}q_y(y-y') - \mathrm{i}q_z(m-m')a/2] \times \exp[\mathrm{i}q_x(m-m')l] \langle \exp[\mathrm{i}q_x(u_m(y) - u_{m'}(y'))] \rangle.$$

Formula (4) is readily deduced.

Appendix 2. Derivation of the 'sine–Gordon' free energy (34) and of the parameters η, η' and U for $I \gtrsim T_R$

At sufficiently high temperatures the interactions between steps may be ignored if fluctuations of sufficiently short wavelength along y are considered. In particular, moving the cut-off $q_{cy} = q_c$ reduces to a one-dimensional problem. For an isolated chain of N' atoms, the Hamiltonian (20) reduces to

$$\mathscr{H} = W_0 \sum_{y=1}^{N'} (u(y+1) - u(y))^2. \tag{A.6}$$

The average value of the Fourier transform $u_q = N'^{-1/2} \Sigma_y u(y) \mathrm{e}^{\mathrm{i}qy}$ is readily deduced:

$$\langle |u_q|^2 \rangle = 2\, \mathrm{e}^{-\beta W_0}/q^2. \tag{A.7}$$

This is just the value which might be deduced from a free energy of the form

$$\mathscr{F} = \tfrac{1}{2} \sum_q \eta q^2 |u_q|^2 \tag{A.8}$$

with

$$\eta = \tfrac{1}{2} T\, \mathrm{e}^{\beta W_0}. \tag{A.9}$$

However, (A.7) can be deduced from (A.8) only if the discrete nature of the $u(y)$ is ignored. This implies that only the long-wavelength part

$$\tilde{u}(y) = N'^{-1/2} \sum_{q<q_c} u_q\, \mathrm{e}^{-\mathrm{i}qy} = \pi^{-1} \sum_{y'} u(y') \sin[q_c(y'-y)]/(y'-y) \tag{A.10}$$

is considered. The cut-off q_c should be such that $\langle (\tilde{u}(y+\pi/q_c) - \tilde{u}(y))^2 \rangle$ is larger than unity, or

$$q_c \lesssim \kappa = 4\pi^2 \exp(-\beta W_0). \tag{A.11}$$

The reason for the factor $4\pi^2$ will become apparent. The weakness of (A.8) is that the discrete nature of the original model is completely lost. The error related to this approximation can be tested by average values of the form

$$X=\left\langle \exp\left(2i\pi\sum_y p_y\tilde{u}(y)\right)\right\rangle. \tag{A.12}$$

Using (A.10) this expression may be written as a product of factors $\langle\exp(if(y)D(y))\rangle$ where $D(y)=u(y+1)-u(y)$, and the coefficients $f(y)$ depend on the p_y. If βW_0 is large and if the number of non-vanishing p_y is small, $f(y)$ is small and

$$\langle\exp(if(y)D(y))\rangle\simeq 1-2(1-\cos f(y))\,e^{-\beta W_0}\simeq\exp(-f^2(y)\,e^{-\beta W_0}).$$

The final result is

$$X=\exp\left(\sum_{yy'} p_y p_{y'} K(y-y')\right) \tag{A.13}$$

where

$$K(y)=(4e^{-\beta W_0}/q_c)\int_{-\infty}^{\infty} dz\,[z(z-q_c y)/|z(z-q_c y)|]\,\mathrm{si}(z)\,\mathrm{si}(z-q_c y) \tag{A.14}$$

where $\mathrm{si}(z)=\int_{|z|}^{\infty} dx\sin x/x$. In particular, formula (6.241) of Gradshtein and Ryzhik (1965) yields

$$K(0)=-\kappa/\pi q_0. \tag{A.15}$$

In analogy with (34) we wish to reproduce (A.13) using an approximate free energy of the form

$$\mathcal{F}=\sum_{q<q_c}\eta q^2|u_q|^2+\sum_y U(1-\cos 2\pi\tilde{u}(y)). \tag{A.16}$$

To lowest order in U, the quantity (A.12) is given by

$$X=(1/p!)(\beta U/2)^p\sum_{y_1,\ldots,y_p}\exp\left[\pi^2\left(\sum_{yy'}p_y p_{y'}\langle(\tilde{u}(y)-\tilde{u}(y'))^2\rangle_0+\sum_{rr'=1}^{p}\langle(\tilde{u}(y_r)-\tilde{u}(y_{r'}))^2\rangle_0\right.\right.$$
$$\left.\left.-2p\sum_y\sum_{r=1}^{p}p_y\langle(\tilde{u}(y)-\tilde{u}(y_r))^2\rangle_0\right)\right] \tag{A.17}$$

where $p=\Sigma p_y$ is assumed to be positive and $\langle\ldots\rangle_0$ denotes the average value for $U=0$. In the special case $p_y=\delta_{y,0}$, identification of (A.13) and (A.17) yields

$$\beta U\sum_{y=-\infty}^{\infty}\exp[-2\pi^2\langle(\tilde{u}(y)-\tilde{u}(0))^2\rangle_0]=\exp(K(0)). \tag{A.18}$$

Using (A.10) and (A.6), relations (A.18) and (A.15) yield after some calculation

$$U\simeq 2\pi T(q_c/\kappa)^{1/2}\exp(-\kappa/\pi q_c)\,e^{-\beta W_0}. \tag{A.19}$$

In the particular case $p_y=p\delta_{y,0}$, X is of order U^{p^2} according to (A.13) and of order U^p according to (A.17). Thus, the two formulae can only coincide to first order in U, and U should be small. This implies that q_c should be sufficiently smaller than κ.

The approximation (A.16) may be tested on the expression

$$X_2(y)=\langle\exp[2i\pi(\tilde{u}(y)-\tilde{u}(0))]\rangle. \tag{A.20}$$

For small y both (A.13) and (A.17) yield $X_2(y)=\exp(-\kappa|y|)$. For $q_c|y|\gg 1$, (A.17) is not correct, but the correct (and obvious) result $X_2(y)=\langle\exp(2i\pi\tilde{u}(0))\rangle^2$ can of course be obtained from (A.16) to second order in U. For intermediate values of y, the expansion of $X_2(y)$ limited to order U^2 is expected to be an acceptable interpolation. The same conclusion holds for other tests of (A.16) using more complicated quantities of form (A.12).

We conclude that (A.16) is justified qualitatively provided q_c is sufficiently smaller than κ, defined by (A.11). η is given by (A.9) and U is given by (A.18) or, more explicitly, by (A.19).

The approximations of this appendix are correct if the interaction between steps per degree of freedom, namely $w_n\pi/q_c$, is small with respect to T. According to (A.11) this implies that $(w_n/T)\exp(\beta W_0)\ll 1$. Comparison with (30) or (38) shows that T should be large with respect to T_R. Near T_R, the formulae of this appendix are presumably only acceptable qualitatively and q_c must be of the same order as κ.

Appendix 3. Renormalisation and behaviour near T_c

The Hamiltonian associated with the free energy (34) is

$$H=H_0+H_1 \tag{A.21}$$

$$H_0=\tfrac{1}{2}\sum_{|q|<q_c}(\tilde{\eta}q_y^2+\tilde{\eta}'q_x^2)|u_q|^2 \tag{A.22}$$

$$H_1=-\tilde{V}_0\int dy\sum_m\cos 2\pi\tilde{u}_m(y) \tag{A.23}$$

where $\tilde{\eta}=\eta/T$ with similar definitions for $\tilde{\eta}'$ and $\tilde{V}_0$.

Let $\tilde{u}_m(y)$ be defined by (33) for a given cut-off and let $\tilde{u}'_m(y)$ be the corresponding quantity for smaller values of q_{cx}, q_{cy}. The effective Hamiltonian for the new variables can be obtained by a cumulant expansion. Keeping terms up to second order in $\tilde{V}_0$ we obtain

$$H(b)=H_0(b)+\Delta H(b) \tag{A.24}$$

where $H_0(b)$ is given by an expression like (A.22) but with smaller cut-offs $q'_{cx,y}=q_{cx,y}b^{-1}$, and

$$\Delta H(b)=\langle H_1\rangle_b-\tfrac{1}{2}(\langle H_1^2\rangle_b-\langle H_1\rangle_b^2). \tag{A.25}$$

The averages are taken over the high-$\boldsymbol{q}$ components of the field with a distribution $P\propto\exp(-H_0)$. The cumulants are easily calculated:

$$\langle H_1\rangle_b=-\tilde{V}_0\int\rho\,dy\sum_m\cos 2\pi\tilde{u}'_m(y)\exp(-2\pi^2\langle u_m^2(y)\rangle_b) \tag{A.26}$$

$$\langle H_1^2\rangle_b-\langle H_1\rangle_b^2=\tilde{V}_0^2\sum_{mm'}\int\int dy\,dy'\cos 2\pi(\tilde{u}'_m(y)-\tilde{u}'_{m'}(y'))(\exp[-2\pi^2\langle(\tilde{u}_m(y)$$

$$-\tilde{u}_{m'}(y'))^2\rangle_b]-\exp(-4\pi^2\langle u_m^2(y)\rangle_b)). \tag{A.27}$$

A term proportional to $\cos 2\pi(\tilde{u}'_m(y)+\tilde{u}'_{m'}(y'))$ has been neglected in (A.27). This is justified as it can be shown that this term is irrelevant near the fixed point of the renormalisation group transformation to be derived below.

The averages in equations (A.26) and (A.27) are easily evaluated for infinitesimal $\ln b$:

$$\langle \tilde{u}_m^2(y)\rangle_b = (1/2\pi\sqrt{\tilde{\eta}\tilde{\eta}'}) \ln b \tag{A.28}$$

$$\langle (\tilde{u}_m(y)-\tilde{u}_0(0))^2\rangle_b = (1/\pi\sqrt{\tilde{\eta}\tilde{\eta}'})(1-J_0(\rho)) \ln b \tag{A.29}$$

where J_0 is the Bessel function of the first kind and

$$\rho = [y^2(\tilde{\eta}'/\tilde{\eta})^{1/2} + m^2(\tilde{\eta}/\tilde{\eta}')^{1/2}]^{1/2}. \tag{A.30}$$

Expanding in Fourier series the difference $(\tilde{u}'_{m'}(y)-\tilde{u}'_{m'}(y'))$ in (A.27) and keeping terms up to order q^2 (A.25) reduces to

$$\Delta H(b) = \tfrac{1}{2} \sum_{|q|<q_{c/b}} (\delta\tilde{\eta}(b)q_y^2 + \delta\tilde{\eta}'(b)q_x^2)|u'_q|^2 - \delta\tilde{V}_0(b) \sum_m \int \mathrm{d}y \cos 2\pi\tilde{u}'_m(y) \tag{A.31}$$

with

$$\delta\tilde{\eta}(b) = (2\pi^3/\tilde{\eta}')\tilde{V}_0^2 \alpha \ln b \tag{A.32}$$

$$\delta\tilde{\eta}'(b) = (2\pi^3/\tilde{\eta})\tilde{V}_0^2 \alpha \ln b \tag{A.33}$$

$$\delta\tilde{V}_0(b) = -\tilde{V}_0(\pi/\sqrt{\tilde{\eta}\tilde{\eta}'}) \ln b \tag{A.34}$$

and the constant

$$\alpha = \pi \int_0^1 r^3 J_0(r)\, \mathrm{d}r \approx \tfrac{1}{3}\pi.$$

Finally, rescaling the length unit and the field to restore the cut-off to its original value we obtain the renormalisation group equations in differential form:

$$\partial\tilde{V}_0/\partial l = [2-(\pi/\sqrt{\tilde{\eta}\tilde{\eta}'})]\tilde{V}_0 \tag{A.35}$$

$$\partial\tilde{\eta}/\partial l = \tfrac{2}{3}\pi^4\tilde{V}_0^2/\tilde{\eta}' \tag{A.36}$$

$$\partial\tilde{\eta}'/\partial l = \tfrac{2}{3}\pi^4\tilde{V}_0^2/\tilde{\eta} \tag{A.37}$$

where l is defined as $b = \mathrm{e}^l$. The quantity (3) does not appear in this appendix so that no confusion is possible.

Equations (A.35)–(A.37) are the generalisation to the anisotropic case of the equations for the isotropic sine–Gordon model derived by other authors (Ohta and Kawasaki 1978).

It can be seen that the ratio $(\tilde{\eta}/\tilde{\eta}')$ remains invariant under a change in length scale. Then (A.36) and (A.37) can be combined to give a single equation for the geometric mean,

$$K = \sqrt{\tilde{\eta}\tilde{\eta}'}, \tag{A.38}$$

which reduces the system of equations to

$$\partial\tilde{V}_0/\partial l = (2-\pi/K)\tilde{V}_0 \tag{A.39}$$

$$\partial K/\partial l = \tfrac{2}{3}\pi^4\tilde{V}_0^2/K. \tag{A.40}$$

Linearising about the fixed point $K=\frac{1}{2}\pi$, $\tilde{V}_0=0$ we finally obtain

$$\partial x^2/\partial l=-2xZ^2 \tag{A.41}$$

$$\partial Z^2/\partial l=-2xZ^2 \tag{A.42}$$

where

$$x=\pi/K-2 \tag{A.43a}$$

$$Z=(4\pi/\sqrt{5})V_0. \tag{A.43b}$$

From (A.41) and (A.42) we deduce that (Ohta and Kawasaki 1978)

$$x^2(l)-Z^2(l)=\text{constant} \tag{A.44}$$

where the constant is independent of l and vanishes at T_R. It is convenient to choose l such that $q_{cy}=\lambda\kappa\approx\kappa$, and $\tilde{q}_{cx}=\pi$. Then V_0 is given by (A.19). It should be noted that, in the present appendix, renormalised length units have been used, i.e., there is one degree of freedom per unit area. In appendix 2 physical length units were used, so that the relation between V_0 and the quantity (A.19) is $V_0=(\pi/q_c)U/T\approx(2\sqrt{\lambda})^{-1/2}\exp(-1/\lambda\pi)$.

T_R can be evaluated from (A.44). The constant vanishes, Z is given by (A.43b) and x is given by (A.43a) where $\eta\eta'$ is the product of expressions (A.9) and (36). The result is

$$(w_n/T_R)\exp(W_0/T_R)=\tfrac{1}{2}\pi^2[1+(\pi/\sqrt{5\lambda})\,e^{-1/\pi\lambda}]^{-2}\approx 1. \tag{A.45}$$

The right-hand side varies from 0.6 to 2 when λ varies from $1/\pi$ to π. The correction to (38) is huge, so that only the order of magnitude is reliable; this is the same as in (30).

Away from the critical point we can expand the right-hand side of (A.44) in powers of the deviation from the critical temperature. To linear order

$$x^2(l)-Z^2(l)=\alpha(T-T_R)/T_R \tag{A.46}$$

where the constant

$$\alpha=8\pi W_0/\sqrt{5}T_R. \tag{A.47}$$

Above T_R Z is irrelevant and (A.41) and (A.42) can be integrated up to $l=\infty$. Then the correlation function can be calculated by equation (25) with $V_\infty=0$. We then obtain

$$\Gamma(\rho)=\langle(\tilde{u}_m(y)-\tilde{u}_m(0))^2\rangle\approx(T/\pi\sqrt{\eta\eta'})\int_0^{p_1}(\mathrm{d}p/p)(1-J_0(p\rho)) \tag{A.48}$$

where ρ is given in (A.30) and p_1 is a cut-off of order $\sqrt{\eta\eta'}$.

$$\partial\Gamma(\rho)/\partial\rho\sim(T/\rho\pi\sqrt{\eta\eta'})\int_0^\infty J_1(x)\,\mathrm{d}x=T/\rho\pi\sqrt{\eta\eta'}. \tag{A.49}$$

Integration yields

$$\Gamma(\rho)=(T/\pi\sqrt{\eta\eta'})\ln\rho+\text{constant} \tag{A.50}$$

where the constant is not universal. At T_R (A.43) and (A.44) give

$$\Gamma_R(\rho)=2\ln\rho/\pi^2. \tag{A.51}$$

Formula (A.51) coincides with (46), which is thus proven to be correct.

Below T_R Z is relevant and iterations of the RG equations take the variables outside the range of validity of (A.41) and (A.42). Thus renormalisation should stop when deviations from the fixed-point behaviour become significant. The solutions of (A.41) and (A.42) below T_R are

$$x(l)=\sqrt{|t|}\,\tan(\Phi_0-\tfrac{1}{2}l\sqrt{\alpha|t|}) \tag{A.52}$$

$$Z(l)=\sqrt{|t|}\,\sec(\Phi_0-\tfrac{1}{2}l\sqrt{\alpha|t|}) \tag{A.53}$$

where Φ_0 is a constant and $|t|=(|T-T_R|/T_R)\alpha$. Inverting (A.52) we find

$$l=(2/\sqrt{|t|})\,[\tan^{-1}(x(0)/\sqrt{|t|})-\tan^{-1}(x(l)/\sqrt{|t|})]. \tag{A.54}$$

For $T\to T_R^-$, $x(0)$ is positive, but the renormalisation group equations take it through negative values. Stopping the iteration when $x(l^*)=-|x(l^*)|$, with $|x(l^*)|<2$, we obtain from (A.54) as $|t|\to 0$

$$l^*\approx 2\pi/\sqrt{|t|}. \tag{A.55}$$

At this point (A.44) yields $Z^2(l^*)\approx x^2(l^*)=O(1)$. Then we can apply the harmonic formulae to the renormalised problem since we are well outside the critical region. The result is

$$\Gamma(\rho)\sim(T/\pi\sqrt{\eta^*\eta'^*})\int_0^{p_1}[p\,\mathrm{d}p/(p^2+\xi^{-2})](1-J_0(p\rho)) \tag{A.56}$$

where p_1 is a cut-off of order $e^{l^*}(\eta^*\eta'^*)^{1/4}$ and the correlation length

$$\xi\approx=(1/2\pi)\,e^{l^*}(\eta^*\eta'^*)^{1/4}V_0^{*-1/2}. \tag{A.57}$$

The integral (A.56) is easily evaluated. For $\rho\gg\xi$ and $T\to T_R^-$

$$\Gamma(\rho)=(2/\pi^2)[|t|^{-1/2}-(\sqrt{\pi\xi/2\rho})\exp(-\rho/\xi)]. \tag{A.58}$$

Appendix 4

Using the Poisson formula expression (34) is transformed into the sum of integrals

$$I'=\sum_{\nu=-\infty}^{\infty}\int\int \mathrm{d}m\,\mathrm{d}y\,\rho^{-\tau}\exp[iq_y y+im(q_x l+\tfrac{1}{2}q_z a+2\pi\nu)]=\sum I_\nu \tag{A.59}$$

where

$$\tau=Tq_x^2/2\pi\sqrt{\eta\eta'} \tag{A.60}$$

and ρ is given by (31). It is convenient to introduce the notation

$$P_x=(q_x l+\tfrac{1}{2}q_z a+2\pi\nu)(\eta'/\eta)^{1/4}.$$

The νth integral in (A.59) may be written as

$$I_\nu=2\pi\int_0^{\infty}\rho^{1-\tau}J_0(P\rho)\,\mathrm{d}\rho$$

where $P=\sqrt{P_x^2+p_y^2}$ and p_y is given by (29*b*). I_ν is the limit, for $\varepsilon\to 0$, of

$$I_\nu(\varepsilon)=2\pi\int_0^\infty \mathrm{e}^{-\varepsilon\rho}\,\rho^{1-\tau}J_0(P\rho)\,\mathrm{d}\rho$$
$$=2\pi\Gamma(2-\tau)(P^2+\varepsilon^2)^{(\tau/2)-1}F(1-\tfrac{1}{2}\tau,\tfrac{1}{2}(\tau-1);1;\tau^2/(\tau^2+\varepsilon^2)).$$

Formula (6.621) of Gradshtein and Ryzhik (1965) has been applied. It is correct only if τ is smaller than 2. For $P\neq 0$ and $\varepsilon\simeq 0$ the argument $P^2/(P^2+\varepsilon^2)$ of the hypergeometric function may be replaced by 1. Using formula (9.122.1) and (8.335.1) of Gradshtein and Ryzhik (1965) we find

$$I_\nu(\varepsilon)=[\Gamma(2-\tau)/\Gamma(\tau/2)\Gamma[\tfrac{1}{2}(3-\tau)]](P^2+\varepsilon^2)^{-1+\tau/2}.$$

Formula (48) results for $\tau\neq 0$. For $\tau=0$, the intensity is 0 for $P\neq 0$, as it should be.

References

Abraham D B 1983 *Phys. Rev. Lett.* **51** 1279
Amit D J, Goldschmidt Y Y and Grinstein G 1980 *J. Phys. A: Math. Gen.* **13** 585
Armand G and Manson J R 1979 *Surf. Sci.* **80** 532
Baxter R J 1982 *Exactly Solved Models in Statistical Mechanics* (London: Academic)
Blatter G 1984 *ETH Preprint*
Bol'shov L A, Pokrovski V L and Uimin G V 1984 *Landau Institute Preprint*
Burton W K and Cabrera N 1949 *Discuss. Faraday Soc.* **5** 33
Chui S T and Weeks J D 1976 *Phys. Rev.* B **14** 4978
Desjonquères M C 1976 *PhD Thesis* Grenoble
—— 1980 *J. Physique Coll.* **41** C3 243
Domb C 1974 *Phase Transitions and Critical Phenomena* ed. C Domb and M S Green vol. 3 p 371 (London: Academic)
Garcia N, Celli V and Nieto-Vesperinas M 1979 *Opt. Commun.* **30** 279
Garcia N, Maradudin A A and Celli V 1982 *Phil. Mag.* A **45** 287
Garibaldi U, Levi A C, Spadacini R and Tommei G E 1975 *Surf. Sci.* **48** 649
Gordon M B and Villain J 1979 *J. Phys. C: Solid State Phys.* **12** L151
Gorse D, Salanon B, Kara A, Fabre F, Perreau J, Armand G and Lapujoulade J 1984 to be published
Gradshtein I S and Ryzhik I M 1965 *Table of Integrals, Series and Products* (New York: Academic)
Gruber E E and Mullins W W 1967 *J. Phys. Chem. Solids* **28** 875
Haldane F D M 1980 *Phys. Rev. Lett.* **45** 1358
Haldane F D M and Villain J 1981 *J. Physique* **42** 1673
Hill N R and Celli V 1978 *Surf. Sci.* **75** 577
Johnson J D, Krinski S and McCoy B M 1973 *Phys. Rev.* A **8** 2526
José J V, Kadanoff L P, Kirkpatrick S and Nelson D R 1977 *Phys. Rev.* B **16** 1217
Knops H J F and den Ouden L W J 1980 *Physica* A **103** 597
Lapujoulade J 1981 *Surf. Sci.* **108** 526
Lapujoulade J, Perreau J and Kara A 1983 *Surf. Sci.* **129** 59
Lau K H and Kohn W 1977 *Surf. Sci.* **65** 607
—— 1978 *Surf. Sci.* **75** 69
Levi A C 1984 submitted to *Surf. Sci.*
Levi A C, Spadacini R and Tommei G E 1981 *Surf. Sci.* **108** 181
—— 1982 *Surf. Sci.* **121** 504
Levi A C and Suhl H G 1979 *Surf. Sci.* **88** 133
Lyuksyutov I F, Medvedev V K and Yakovkin 1981 *Zh. Eksp. Teor. Fiz.* **80** 2452
Mayer H D 1981 *Surf. Sci.* **104** 117
Ohta T 1978 *Prog. Theor. Phys.* **60** 968
Ohta T and Kawasaki K 1978 *Prog. Theor. Phys.* **60** 365

Pokrovskii V L and Talapov A L 1980 *Zh. Eksp. Teor. Fiz.* **78** 269
—— 1984 *Theory of Incommensurate Crystals (Soviet Scientific Reviews, Physics)* vol. 1 (Chur: Harwood) pp 11–2
Schulz H J 1984 *Workshop on Colloidal Crystals, Les Houches* unpublished
Tommei G E, Levi A C and Spadacini R 1983 *Surf. Sci.* **125** 312
Villain J and Bak P 1981 *J. Physique* **42** 657
Weeks J D 1980 *Ordering in Strongly Fluctuating Condensed Matter Systems* ed. T Riste (New York: Plenum) p 293
Wiegmann P B 1978 *J. Phys. C: Solid State Phys.* **11** 1583
Zaremba E and Kohn W 1976 *Phys. Rev.* B **13** 2270